Scattering Transform of Heart Rate Variability for the Prediction of Ischemic Stroke in Patients with Atrial Fibrillation

Roberto Leonarduzzi[1], Patrice Abry[1], Herwig Wendt[2], Ken Kiyono[3],
Yoshiharu Yamamoto[4], Eiichi Watanabe[5], Junichiro Hayano[6]

[1]Univ Lyon, Ens de Lyon, Univ Claude Bernard, CNRS, Laboratoire de Physique, F-69342 Lyon, France;
[2]IRIT, CNRS UMR 5505, University of Toulouse, France;
[3]Division of Bioengineering, Graduate School of Engineering Science, Osaka Uinversity, Toyonaka, Japan;
[4]Educational Physiology Laboratory, Graduate School of Education, University of Tokyo, Tokyo, Japan;
[5]Dept of Cardiology, Fujita Health University School of Medicine, Toyoake, Japan;
[6]Dept of Medical Education, Nagoya City University Graduate School of Medical Sciences, Nagoya, Japan;

Abstract

Atrial fibrillation is an identified risk factor for ischemic strokes. Thus, the dynamics of heart rate under fibrillation might provide a useful predictor for strokes. The complex, nonlinear and multiscale nature of the heart rate calls for the use of powerful signal processing techniques. We explored the application of a novel tool, the scattering transform, to discriminate and predict ischemic strokes from heart rate dynamics. We found that groups of scattering coefficients, at several time scales, were significantly higher (p-value < 0.05) in patients who developed ischemic strokes than in those who did not. We also found significant differences in predictive power (C-statistic) between scattering coefficients and the CHA_2DS_2-VASc score. Results suggest the use of scattering coefficients for the analysis of patients with atrial fibrillation.

Keywords *Atrial fibrillation, ischemic stroke, heart rate variability, scattering transform, multiscale analysis.*

1 Introduction

Atrial fibrillation. AF is a supraventricular tachyarrythmia characterized by uncoordinated atrial activation [1]. In this condition, the sinus node loses its ability to govern ventricular response [2], and, instead, the atrium is depolarized by a chaotic pattern of rapid and random impulses with two main consequences. First, the atrial tissue contracts in an unsynchronized and erratic way, causing the atrial wall to quiver rather than contract [1]. Second, the random pulses that reach the atrioventricular node cause high irregularity in the ventricular response RR intervals [3]. In consequence, the ventricular response is characterized by a white-noise-like nature in the high and low frequency bands (2.5 s to 25 s), and more complex and organized dynamics in the very-low and ultra-low bands (25 s to more than 300 s), which reflect circadian rhythms and AV node properties mediated by the autonomous nervous system [1, 2].

Ischemic stroke. The impaired mechanical function of the atrium decreases blood flow rates within, and thus favors thrombus' formation and embolic events [1]. Thus, AF is identified as an important risk factor for ischemic strokes (IS) [1]. In fact, treatment of AF patients with oral anticoagulants is a mainstay of current clinical practice [1]. In consequence, a robust risk stratification scheme of stroke likelihood in AF patients would be of great clinical value, aiding in the decisions for prophylaxis and allowing to reduce the exposure of low-risk patients to bleeding complications.

Related work. To date, a standard risk stratification metric to guide antithrombotic therapy in AF patients is provided by the CHA_2DS_2-VASc score [4]. This score groups many risk factors: congestive heart failure, hypertension, age ≥ 75 years (doubled), diabetes, stroke (doubled), vascular disease, age 65–74 years, and gender [4]. On a different approach, risk factors have been obtained from the irregular dynamics of the ventricular response RR intervals, since their irregularity shares a common origin with atrial mechanisms that favor thrombogenesis. In [5], the authors used traditional time-domain statistical measures and entropies to characterize irregularity, and showed that they are associated with an increased risk of mortality. More recently, an explicit connection between irregular RR-interval dynamics and IS was explored in [6], where the authors showed that multiscale sample entropy constitutes a useful predictor of ischemic strokes from AF patients.

Goals, contributions and outline. In this contribution, we propose to explore the potential of a recently introduced signal processing tool to predict ischemic strokes from the RR interval irregularity of AF patients. This tool, referred to as the scattering transform [7, 8], is a nonlinear multiscale transform that provides a stable and informative characterization for processes with complex multiscale dynamics. It has been successfully used, e.g., for audio classification [8] and acidosis detection from

This work was supported by CNRS grant PICS 7260.

fetal heart rate [9–11]. A brief introduction to the scattering transform is provided in Sec. 2. A database of 173 AF patients from a hospital in Aichi, Japan, is then described in Sec. 3. Next, the potentials and benefits of the scattering transform for prediction of ischemic strokes from AF patients are discussed in Sec. 4.

2 Scattering transform

Wavelet coefficients. Let $X(t)$ denote the signal to be analyzed. Let also $\psi(t)$ denote a complex analytic mother wavelet, that is, a band-pass filter supported over positive frequencies. Let $\psi_j(t) = \{2^{-j}\psi(2^{-j}t) \;\; j \in \mathbb{N}\}$ denote the collection of templates of ψ dilated at scales 2^j. The complex dyadic wavelet transform computes the downsampled convolutions $X \star \psi_j(2^j k)$ for all times $t = 2^j k$ and scales 2^j.

Scattering transform. First-order scattering coefficients $S_1(j_1)$ are defined as the average amplitude of the modulus of wavelet coefficients $X \star \psi_{j_1}(t)$, for any $1 \leq j_1 \leq J$:

$$S_1(j_1) = 2^{-j_1} \sum_{k=1}^{2^{j_1}} |X \star \psi_{j_1}(2^j k)|. \qquad (1)$$

The average in (1) looses all information related to the time evolution of $|X \star \psi_j(t)|$. This information can be recovered by computing a second level of wavelet coefficients: $|X \star \psi_{j_1}(t)| \star \psi_{j_2}(t)$, for all scales 2^{j_2} such that $j_1 \leq j_2 \leq J$. Since their amplitude is proportional to that of previous level coefficients, they need to be renormalized to avoid spurious dependence. Thus, second-order scattering coefficients are defined, for $j_2 > j_1$, as:

$$S_2(j_1, j_2) = \frac{2^{-j_2}}{S_1(j_1)} \sum_{k=0}^{2^{j_2}} ||X \star \psi_{j_1}| \star \psi_{j_2}(2^{j_2} k)|. \qquad (2)$$

Interpretation. Second-order coefficients can be interpreted as providing a nonlinear representation of the multiscale dynamics of the wavelet coefficients of X at scale j_1. In this work we focus only on the first two orders of scattering coefficients, since they carry most of the energy in X, as shown in [7, 9]. Information contained in first-order scattering coefficients $S_1(j_1)$ is related to the second-order statistics (correlation, spectrum) of X [7], and thus called *linear* in the following. In contrast, second-order scattering coefficients depend on the higher-order moments of X (and thus characterize X beyond spectral properties) [7, 9], and will thus be termed *nonlinear*.

Illustration. Fig. 1 illustrates this property of scattering coefficients. It shows the (log of) coefficients $S_1(j_1)$ and $S_2(j_1 = 10, j_2)$, averaged over realizations of fractional Gaussian noise (fGn, [12]), a processes defined entirely by its second order moments, and the increments of multifractal random walk (MRW, [13]), a process with nontrivial higher-order statistics. Realizations of both processes where synthesized to have the exact same covariance structure. In consequence, Fig. 1 (left) shows that linear scattering coefficients $S_1(j_1)$ are unable to distinguish both processes. In contrast, Fig. 1 (right) shows that

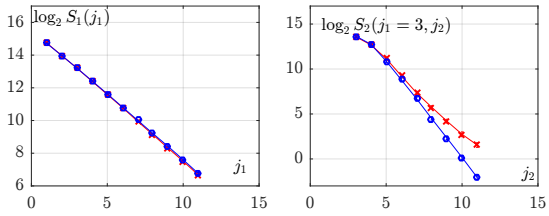

Figure 1: Coefficients $\log_2 S_1(j_1)$ (left) and $\log_2 S_2(j_1 = 3, j_2)$ (right), for two synthetic processes with the same second-order moments but different higher-order moments.

nonlinear coefficients $S_2(j_1, j_2)$, for a particular choice of j_1, are able to discriminate them based on their higher-order statistics.

Software. We computed scattering coefficients using the ScatNet software package for Matlab, available at `http://www.di.ens.fr/data/software/scatnet/`, using a Morlet analytic wavelet.

3 Database

Data collection. We analyzed 24-hour Holter records from patients suffering from permanent AF, defined as AF of more than one year of duration, with no evidence of sinus rhythm, and with no planned sinus rhythm restoration. We excluded patients with complete AV block, sustained ventricular tachycardia, ventricular ectopy $> 5\%$, cardiac pacemakers, paroxysmal AF, valvular AF or prosthethic heart valves, with more than 5% of the Holter record corrupted by artifacts or noise, taking rhythm control drugs, or that had acute coronary syndrome, strokes, hemodynamic instability or undergone surgery in the preceding 6 months. Application of these criteria led to a total of 173 subjects. The CHA_2DS_2-VASc score was recorded for each patient as a baseline measurement of the stroke risk [4].

Patients underwent a follow-up period of 47 ± 35 months. During this period, the diagnosis of ischemic stroke was made by a neurosurgeon. Ischemic strokes were observed in 22 patients.

The study was approved by the ethics committee of Fujita Health University and conformed to the principles outlined in the declaration of Helsinki. All patients provided written informed consent at the time of Holter recording.

Recordings. The 24-hour-long Holter ECGs were recorded with a 2-channel digital recorder (Fukuda Denshi, Tokyo) and digitized at a 125 Hz sampling frequency and 12 bit resolution. RR-intervals were detected automatically, with a manual review and edition by experts.

Preprocessing. All RR time series were preprocessed for outliers, excluding all RR intervals smaller than 350 ms, and larger than 3500 ms or 2.5 times the local 90% percentile. Then, each RR time series was interpolated and resampled at 2 Hz with a linear interpolation scheme, since the wavelet procedure that we applied requires a uniformly sampled time series.

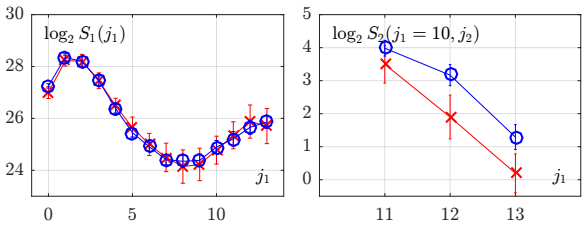

Figure 2: Coefficients $\log_2 S_1(j_1)$ (left) and $\log_2 S_2(j_1 = 10, j_2)$ (right), for the RR time series of patients that did (red crosses) and did not (blue crosses) develop ischemic strokes (median and 95% confidence intervals).

Clinical information. All records are complemented by clinical information, including the reference CHA_2DS_2-VASc score and the administration of antithrombotic drugs such as warfarin and antiplatelet agents.

4 Results and discussion

Scattering coefficients. Fig. 2 shows the linear S_1 (left) and nonlinear S_2 (right, for $j_1 = 10$) scattering coefficients for patients that did (red crosses) and did not (blue circles) develop ischemic strokes. S_1 is remarkably similar for both classes and thus unsuitable for discrimination. In contrast, S_2 shows significant differences between the classes for several values of j_1 and j_2. Fig. 2 (right) shows the particular case for $j_1 = 10$, where coefficients $S_2(10, j_2)$ are clearly able to discriminate between classes. Notably, patients that developed IS show smaller values for S_2, indicating that their heart rate dynamics are characterized by less nonlinear variability.

It is worth noticing that, interestingly, S_1 reproduces the spectral behavior documented in [2]: the existence of two scaling regimes, for $j \in [2, 8]$ and $j \in [9, 13]$. The cutoff scale is $j_c = 8 \approx 2$ min, also in agreement with findings in [2, 6]. The loss of scaling for $j_1 < 2$ is due to the effects of the interpolation and digitalization, which are limited to fine scales.

Statistical analysis. To assess the ability of scattering coefficients to distinguish between the two classes, we performed individual Wilcoxon ranksum tests on each $\log_2 S_1(j_1)$, for all j_1, and each $\log_2 S_2(j_1, j_2)$, for all j_1 and j_2. Further, we grouped significant neighboring coefficients at contiguous scales j_2 for fixed j_1. The scales j_1 and j_2 involved in these groups are indicated in Table 1. We averaged all (log-transformed) coefficients in such groups to obtain discriminant statistics, and performed Wilcoxon ranksum tests on these groups as well.

Table 1 reports the p-values (for the sake of space, only the significant groups are shown). Further, Fig. 3 shows boxplots for each group and class. It can be seen that statistically significant differences can be found on the second-order coefficients computed from a wide range of time scales 2^{j_1} (ranging from ≈ 2 s for $j_1 = 2$, to ≈ 512 s for $j_1 = 10$).

Note that group SG4 is related to the dynamics of RR intervals in the ultra low frequency range (including time scales larger than 8.5 min). However, groups SG1, SG2 and SG3 indicate that scattering coefficients are also found to be significant *at smaller time scales*, ranging from ≈ 2 s ($j_1 = 2$) to ≈ 2 min. Notably, scattering coefficients are not found to be significant in the very low frequency range, where multiscale entropy was found to be significant in [6].

Table 1: Definition of groups and p-values.

Group	j_1	j_2	p-value
SG1	2 (2 s)	$[5, 7]$ ($[16$ s , 1 min $]$)	0.039
SG2	3 (4 s)	$[5, 8]$ ($[16$ s , 2 min $]$)	0.048
SG3	4 (8 s)	$[5, 8]$ ($[16$ s , 2 min $]$)	0.005
SG4	10 (8.5 m)	$[11, 13]$ ($[17$ min , 1 h $]$)	0.022

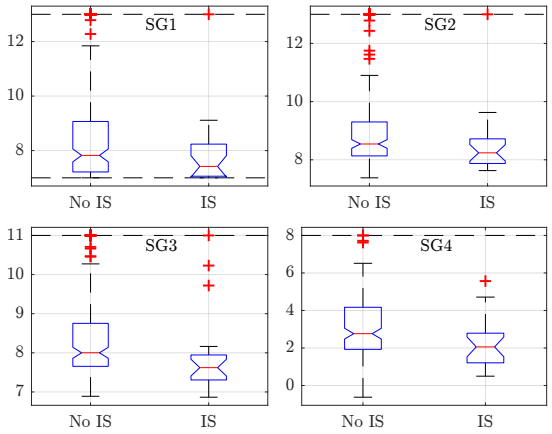

Figure 3: Boxplots of the four groups of scattering coefficients, for patients that did (IS) and did not (no IS) develop an ischemic stroke. Outliers above the dashed line are not displayed.

Correlation. Table 2 shows the Spearman correlation coefficients between each pair of groups. For comparison purposes, multiscale entropy in the very low frequency range ($\text{MeanEn}_{\text{VLF}}$, denoted for brevity as EN), proposed in [6], is also included. It can be seen that all groups show very weak correlations. This suggests that all groups measure different aspects of the RR dynamics and provide complementary information. Further, all groups are uncorrelated with EN, which can be expected from the fact that they are computed at different time scales.

Predictive performance. To assess the power of scattering coefficients to predict the occurrence of ischemic strokes, we performed Receiver Operating Characteristic (ROC) analyses on all groups. For comparison purposes, we also analyzed EN and the CHA_2DS_2-VASc score (CHA), as in [6].

Fig. 4 (top) shows the C-statistics for EN, CHA and the four groups of scattering coefficients. It can be seen that, despite an overall modest performance, groups SG3 and SG4, as well as EN, provide a better predictive power than the standard CHA_2DS_2-VASc score.

If the analysis is restricted to patients not receiving antithrombotic treatment (109 subjects), Fig. 4 (bottom, left), predictive performance increases dramatically, with SG4 reaching almost 80%. In contrast, analysis of pa-

Table 2: Spearman correlation for all scattering group and multiscale entropy (EN).

	SG1	SG2	SG3	SG4	EN
SG1		0.268	0.204	0.053	0.039
SG2			0.188	0.03	0.003
SG3				0.035	0.031
SG4					−0.069

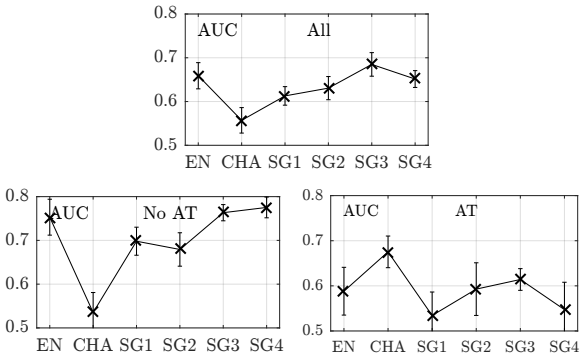

Figure 4: Area under the ROC curve (and 95% confidence intervals computed from 5-fold cross-validation) for multiscale entropy (EN), CHA_2DS_2-VASc score (CHA), and the four groups of scattering coefficients indicated in Table 1. Analysis was performed on all patients (top), and those that did and did not receive antithrombotic treatment (bottom left and right, respectively).

tients under antithrombotic treatment (69 subjects), Fig. 4 (bottom, right), shows that predictive power is poor, and that CHA_2DS_2-VASc is actually the best predictor. This suggests that in these patients the ischemic stroke is actually not associated with AF. Results in this section suggest the promising value of SG3 and SG4, as well as EN, as predictors of ischemic stroke, in particular when patients are not under antithrombotic treatment.

5 Conclusion and future work

In this work, we have made an exploration of the value of scattering coefficients for the prediction of ischemic stroke from patients with atrial fibrillation. Results suggest that scattering coefficients have a good discriminant power, using information from a wide range of time scales and statistical orders. Further, these groups show an acceptable predictive performance, in particular when only patients that are not receiving antithrombotic drugs are considered. Future work will address the improvement of predictive power by the joint use of all the uncorrelated predictors considered here, with an adequate machine learning strategy. Moreover, the exploration of complementary nonlinear features will also be considered.

References

[1] V. Fuster, et al. ACC/AHA/ESC 2006 Guidelines for the Management of Patients With Atrial Fibrillation A Report of the American College of Cardiology/American Heart Association Task Force on Practice Guidelines and the European Society of Cardiology Committee for Practice Guidelines. *Circulation*, 114(7):e257–e354, 2006.

[2] J. Hayano, et al. Spectral characteristics of ventricular response to atrial fibrillation. *Am. J. Physiol. Heart Circ. Physiol.*, 273(6):H2811–H2816, 1997.

[3] J. A. Kirsh, et al. Ventricular response to atrial fibrillation: role of atrioventricular conduction pathways. *J. Am. Coll. Cardiol.*, 12(5):1265–1272, 1988.

[4] G. Y. Lip, et al. Identifying Patients at High Risk for Stroke Despite Anticoagulation A Comparison of Contemporary Stroke Risk Stratification Schemes in an Anticoagulated Atrial Fibrillation Cohort. *Stroke*, 41(12):2731–2738, 2010.

[5] A. Yamada, et al. Reduced ventricular response irregularity is associated with increased mortality in patients with chronic atrial fibrillation. *Circulation*, 102(3):300–306, 2000.

[6] E. Watanabe, et al. Multiscale Entropy of the Heart Rate Variability for the Prediction of an Ischemic Stroke in Patients with Permanent Atrial Fibrillation. *PLOS ONE*, 10(9):e0137144, 2015.

[7] S. Mallat. Group Invariant Scattering. *Comm. Pure Appl. Math.*, 65(10):1331–1398, 2012. arXiv: 1101.2286.

[8] J. Andén and S. Mallat. Deep Scattering Spectrum. *IEEE Trans. Sig. Proc.*, 62(16):4114–4128, 2014.

[9] V. Chudáček, et al. Scattering Transform for Intrapartum Fetal Heart Rate Variability Fractal Analysis: A Case-Control Study. *IEEE Trans. Biomed. Eng.*, 61(4):1100–1108, 2014.

[10] Chudáček, et al. Low dimensional manifold embedding for scattering coefficients of intrapartum fetale heart rate variability. In *Conf Proc IEEE Eng Med Biol Soc*, pages 6373–6376, 2014.

[11] V. Chudáček, et al. Scattering transform for intrapartum fetal heart rate characterization and acidosis detection. In *Conf Proc IEEE Eng Med Biol Soc*, pages 2898–2901, 2013.

[12] B. Mandelbrot and J. Van Ness. Fractional Brownian Motions, Fractional Noises and Applications. *SIAM Review*, 10(4):422–437, 1968.

[13] E. Bacry, J. Delour, and J. F. Muzy. Multifractal random walk. *Phys. Rev. E*, 64(2):026103, 2001.

Address for correspondence:

Patrice Abry
Lab de Physique, ENS de Lyon, Lyon, France
patrice.abry@ens-lyon.fr